

Cowl Deflection Angle in a Supersonic Air Intake

S. Das and J. K. Prasad

Birla Institute of Technology, Mesra, Ranchi-835 215

ABSTRACT

A numerical study for a two-dimensional mixed compression supersonic air intake with different cowl deflections has been made with and without back pressure. Numerical simulations have been made with RANS solver using a k- ω turbulence model. Overall flow field existing inside intake has been captured which indicates the change in flow field with cowl deflection angle. Overall performance has been obtained. Computations have been also made with bleed. The computed data are compared with available experimental and numerical results and indicated a good comparison. Results obtained through the present series of computation indicate an improvement in performance with small cowl deflection which is comparable to performance with 2.8 per cent bleed.

Keywords: Cowl deflection, cowl deflection angle, supersonic air-intake, numerical simulation

NOMENCLATURE

P	Static pressure
P_0	Total pressure
C_α	Cowl deflection angle
L	Overall length of intake
h_c	Capture height of intake
h_d	Height at diffuser exit

Subscripts

i	Freestream condition
e	Exit condition of intake

1. INTRODUCTION

The aerodynamic design of a supersonic intake becomes a critical issue to estimate the overall performance of an air-breathing propulsion system which operates at supersonic to hypersonic speeds and captures the incoming air to supply to combustor of main engine after compression. Combined cycle engines have the advantage of having a single flow passage, where compression could be achieved through a series of oblique shocks generated through compression ramps and internal contraction. This leads

to formation of series of shock waves and expansion waves inside such intakes. The advantage of such a system is the simple geometry and possibility of adopting variable geometry for efficient operation of engine depending upon the flight operating conditions. A schematic of flow field for a typical combined cycle intake is presented in Fig. 1. At the design condition, the series of compression shocks generated by the ramps gets reflected at the tip of the cowl and leads to further compression inside the intake with the formation of terminal shock at the throat of the intake after passing through a series of shocks. Due to the interaction of shock wave and boundary layer, there exists the possibility of flow separation inside the intake and it is likely to reduce the overall performance of the intake. There also exists the possibility that intake may not start or intake buzz may occur due to possible shock oscillations inside the intake. All these flow phenomena might lead to loss of performance or damage to the structures. To alleviate these problems, attempts are being made by adopting various methods like bleeding, variable geometry, side wall compression, perforations, isolators, length of diffuser, etc, to improve the performance of engine. Each

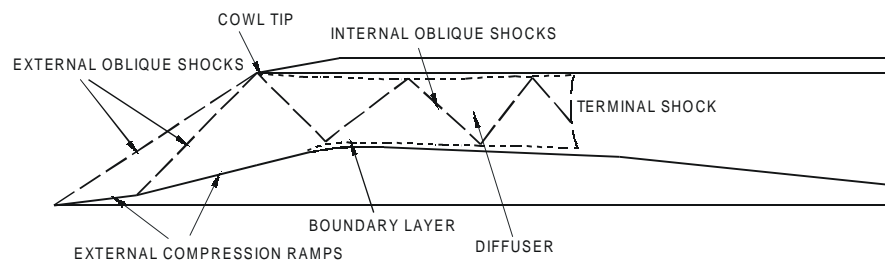


Figure 1. Schematic of flow field.

of the methods has its own merits and demerits as it involves incorporation of additional system e.g., installation of bleed system or movement and control of system, cooling system, etc, for efficient operation over wide range of operations of intake.

Neale and Lamb¹⁻² demonstrated the effect of various geometrical parameters like ramp angle, side wall, geometry variation, diffuser length, Reynolds number, etc on an intake designed for Mach number 2.2, through extensive and systematic experiments. Adopting various numerical techniques, flow oscillations inside the intake due to shocks have been captured numerically by earlier workers Liou³, *et al.*, Hsieh⁴, *et al.*, Biedron⁵, *et al.*, etc. Supersonic mixed compression air intake design using CFD techniques is reported by Valorani⁶, *et al.* The effects of isolator length on flow inside a mixed compression intake are dealt by Reinartz⁷, *et al.*, obtained through computations at hypersonic speed. The start/unstart characteristics of intake has been experimentally investigated by Wie⁸, *et al.*, by changing the cowl length and height, whereas the effect of bending the cowl has been reported by Kubota⁹, *et al.* at hypersonic speed. Oscillations due to flow separation in subsonic diffuser are reported by Fisher¹⁰, *et al.*, Sajben¹¹, *et al.*, Trapier¹², *et al.*, etc.

The objective of the present investigation is to study the flow for a two-dimensional intake configuration used^{1,2} through computations using the commercial software FLUENT. The emphasis was to capture the effect of cowl tip deflection for possibility of adopting this technique as alternative or to support the other methods to improve the performance.

2. GEOMETRICAL DETAILS

To obtain the effect of deflection of cowl, the basic intake geometry used in^{1,2} has been adopted for the present study, primarily due to availability of experimental data. Figure 2 shows the basic geometrical details of intake. It has ramps having angles of 7° and 14° with capture height (h_c) of 63.5 mm. The diverging portion has deflection angle of 2.50 and 6°. Further details are depicted in Fig. 2. For this particular geometry, the cowl has been deflected by angle (C_α), along the local flow direction, such that it leads to reduce the contraction upto the location of throat and further it becomes parallel to free stream direction.

3. COMPUTATIONAL METHODOLOGY

The computations are performed using commercial

software FLUENT which adopts finite volume approach to solve compressible Reynolds Averaged Navier Stokes equations with standard turbulence models. Present computations have been made adopting $k-\omega$ turbulence model. The standard $k-\omega$ model in FLUENT is based on the Wilcox $k-\omega$ model, which is designed to be applied throughout the boundary layer and is applicable to wall-bounded flows as well as free-shear flows. “ $k-\omega$ ” turbulent simulations over air intake reported by Reinartz⁸, *et al.* and Coratekin¹³, *et al.* gave a good comparison with experimental results at supersonic Mach numbers. In the present tests, compressibility corrections were applied and the default model constants were set. Explicit coupled solver with upwind discretisation scheme for flow and transport equations was adopted. For faster convergence, 4-stage multigrid was used. The computational domain was restricted to the internal duct section enclosed by ramp surface and the cowl internal surface only with appropriate boundary conditions to reduce the computational time. Computations were made with distributed uniform quadrilateral cells having minimum spacing in the y -direction near the wall of the order of 0.15 mm and y^+ of 25. Computations were made with three different grids [Grid 1 (69,600 cells), Grid 2 (83,400 cells) and Grid 3 (96,900 cells)]. Figure 3 shows the computed Mach number along the mid-section of the intake for these three grids. Based on this result, it was decided to make further computations with Grid 2. A typical grid distribution adopted near the throat region is shown in Fig. 4.

Boundary conditions at inlet boundary were specified by stagnation and static pressures corresponding to supersonic flow of Mach 2.2 with a small turbulent intensity and viscosity ratio. At the exit, pressure outlet boundary condition was assigned. For supersonic outflow, the variables were extrapolated from the interior cells and for subsonic outflow, a back pressure was enforced. No-slip boundary conditions were enforced at all the solid walls. Computations were made for free flow (i.e., no back pressure) and with a back pressure specified by appropriate subsonic out flow condition.

4. VALIDATION TESTS

Experimental results are reported by Neale and Lamb¹ on a variable geometry two-dimensional intake for different bleed mass flow rates, bleed geometry, and length of the subsonic diffuser. The data available on the configuration for 2.8 per cent of bleed at freestream Mach number 2.2 has been used to validate the present computation. Necessary

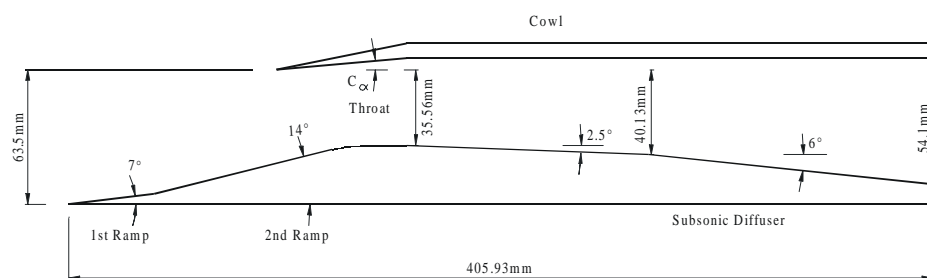


Figure 2. Geometrical details of intake.

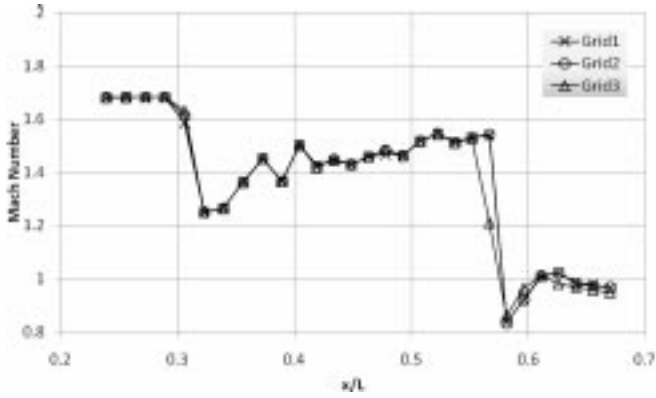


Figure 3. Comparison of centerline mach numbers for three different grid levels.

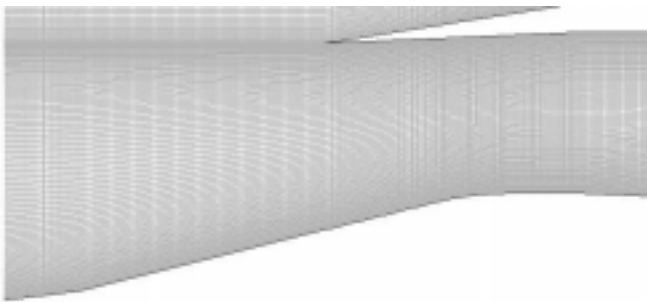


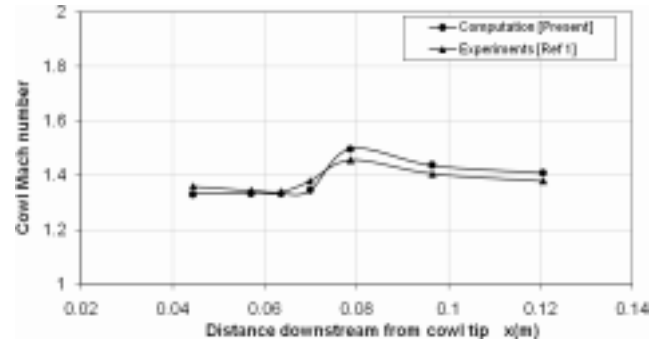
Figure 4. Grid arrangement near the cowl tip and throat.

flow conditions were simulated and computations were made. Comparison of computed Mach number with the experimental result of Neale and Lamb¹ is presented in Fig. 5(a), which indicates fairly good comparison. Typical Mach contour in the vicinity of bleed region is shown in Fig. 5(b).

Computational results on a hypersonic inlet geometry with back pressure is reported in Van⁸, *et al.* to validate the present computations with back pressure, simulations have been made on same geometry of Van⁸, *et al.* with a back pressure which corresponds to 7 times the freestream pressure. Comparison of the pressure distribution along the inner surface of cowl indicates reasonably good agreement which is presented in Fig. 6. This clearly indicates the sufficiency of grid distribution, turbulence model, boundary conditions, etc being used in present computations to capture the flow field details. As the comparison with available experimental and computational results are found to be reasonably good, further computations were made to study the effect of deflection of cowl tip.

5. RESULTS AND DISCUSSION

For obtaining the effect of cowl deflection angle (C_{α}), computations have been made at different cowl deflection angle C_{α} , in the range of 1° to 5° and at freestream Mach number of 2.2. Computations were made for free flow (supersonic flow at exit) as well with back pressure (subsonic flow) at the exit. Results for free flow are presented and



(a)



(b)

Figure 5. (a) Comparison of Mach number distribution with experimental results, and (b) Mach contour in the vicinity of bleed region.

discussed followed by the results obtained for a typical back pressure.

6. COMPUTATION FOR FREE FLOW

To capture the flow field inside the intake, which consists of external oblique shock followed by reflected shock from tip of the cowl and subsequent terrain of shocks along with interaction with boundary layer, computations were made with free exit flow having supersonic flow at exit. The computed pressure distribution on the ramp and inside surface of cowl is presented in Fig. 7 for cowl tip deflection (C_{α}) of 1° . The wall pressure was normalised with free stream pressure. The increase in pressure on

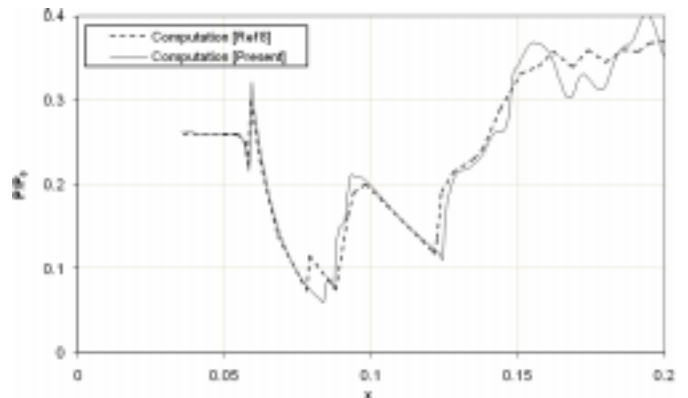


Figure 6. Comparison of pressure distribution on the cowl inner surface with back pressure.

ramp surface at a location of x/L of 0.1 and x/L of 0.34, indicates the presence of shock due to ramp and reflected shock from the cowl tip. Similarly, the pressure jump on the cowl surface at x/L of 0.38 indicates the formation of shock wave at around cowl deflection terminal point. A pressure contour corresponding to this case is presented in Fig. 8, which shows series of shocks inside the inlet and as well supersonic flow at the exit and corroborates well with results presented in Fig. 7.

Further computations were made at different cowl deflection angles (C_α). Figure 9 shows the pressure contour for C_α of 5° . Comparison of Figs 8 and 9 clearly indicates the change in flow field inside the intake due to change in cowl deflection angle. As expected, the location of shock reflected from cowl tip and impinging on the ramp surface has moved downstream. Due to the presence of expansion flow in this region, the possible separated zone has been captured which indicates the complexity of flow field existing inside intake. Further downstream the flow behaviour seems to be similar to the result obtained at C_α of 1° .

The computed pressure distribution on the ramp and cowl surface at different C_α is presented in Figs 10 and 11 showing the effect of cowl deflection. The behaviour of pressure distribution on the ramp surface is similar up to the location of impingement of shock generated by the cowl as expected. With increase in C_α , the location of shock impingement point moves downstreams as could be seen from the observed pressure jump. The movement

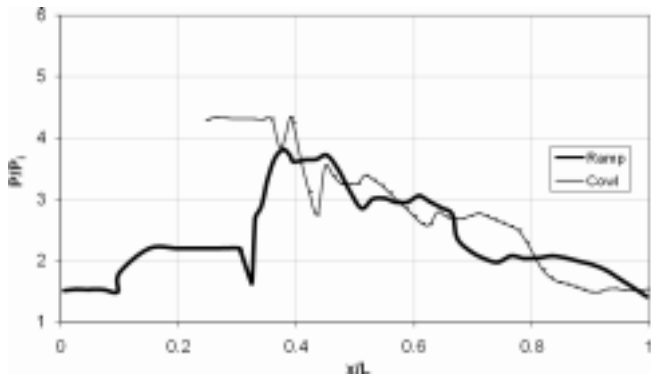


Figure 7. Surface pressure distribution for $C_\alpha = 1^\circ$.



Figure 8. Pressure contours showing the internal duct flow for $C_\alpha = 1^\circ$.



Figure 9. Pressure Contours showing the internal duct flow for $C_\alpha = 5^\circ$.

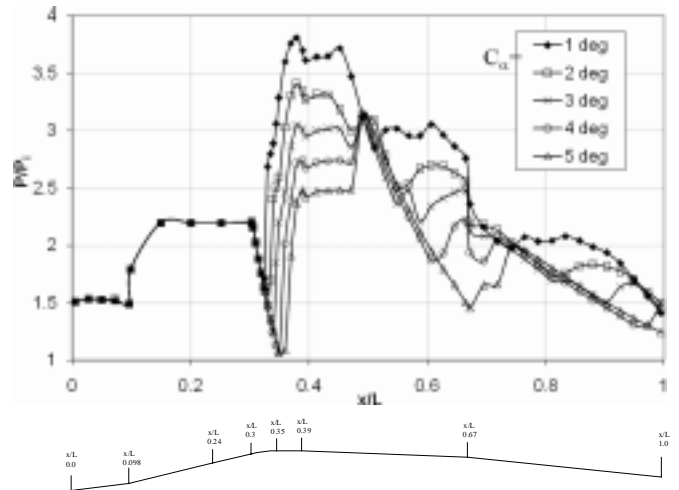


Figure 10. Pressure distribution on ramp surface for various C_α with free flow at the exit.

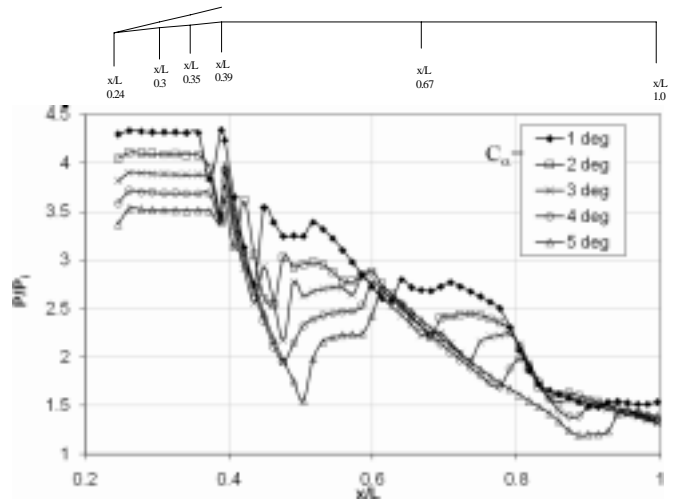


Figure 11. Cowl surface pressure distribution for various C_α with Free flow at the exit.

is of the order of $0.05L$. Similar observation is reported in Kubota⁹, *et al.* based on the experimental results. It is also observed that jump in pressure reduces with increase in C_α , which is expected due to smearing of the shock wave due to shock angle and interaction with boundary layer. Further downstream, the internal flow gets affected indicating that the cowl deflection is likely to change the performance of the intake. With increase in C_α , the separation zone seems to reduce, and hence, improvement in performance could be expected. This is also qualitatively seen from Figs. 8 and 9. The pressure distribution on the cowl surface at different C_α is depicted in Fig. 11, which also indicates the improvement in flow pattern with increase in C_α .

The performance of intake is generally defined with the help of pressure recovery which is defined as ratio of total pressure at exit plane and total pressure of incoming flow. This quantity has been obtained from the computed results and presented in Fig.12. It could be seen that flow is almost uniform except in the vicinity of solid surfaces, which is likely due to the boundary layer. With increase

in C_α , the recovery pressure improves by about 2 per cent. To obtain the overall recovery pressure, averaging of the pressure was made using the pressure distribution presented in Fig. 12, excluding the distribution near the surface. The variation of overall pressure recovery with cowl deflection angle (C_α) is presented in Fig. 13, which indicate the improvement in pressure recovery from 94 per cent to 97 per cent. The pressure recovery was also obtained by making inviscid computation at $C_\alpha=0$ which indicated a value of 94.1 per cent, also shown in Fig. 13. For improvement in pressure recovery, application of bleed has been studied and reported by Neale and Lamb¹. Computations have been also made by providing a bleed of mass of air, near the throat region corresponding to about 2.8 per cent of the captured mass. The computed results indicated a pressure recovery of 95.4 per cent which is also shown in the same figure. This indicates that the improvement in performance achieved with bleed of 2.8 per cent could also be achieved through cowl deflection of about 2° and hence could also be considered as an alternative to improve the overall performance of intake.

7. COMPUTATION OF FLOW WITH BACK PRESSURE

After studying the effect of cowl deflection angle (C_α) on free exit flow, computations were made with a back pressure with the same grids as used for earlier computations.

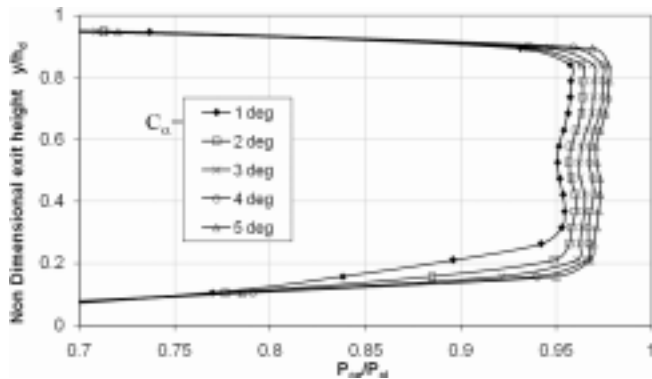


Figure 12. Pressure distribution at various cowl deflection angles.

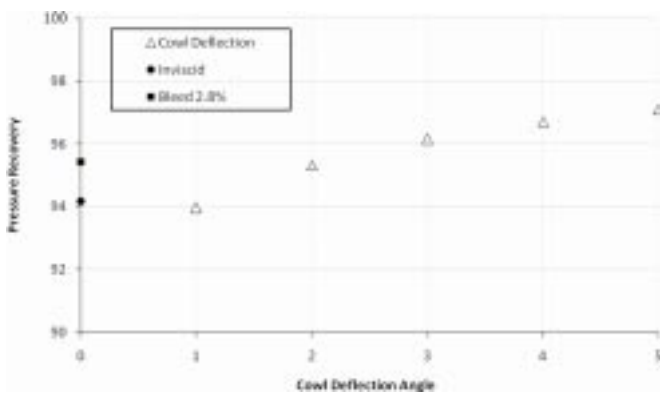


Figure 13. Comparison of pressure recovery for free flow at exit.

For the present computation, a back pressure ratio (P_e/P_0) of 7.0 has been used which corresponds to supercritical operation of intake. The computed results already obtained for free exit flow are used as initial condition for computation with back pressure to save the computation time. Necessary boundary conditions simulating the back pressure at the exit were enforced.

Figure 14 shows the density contour inside the intake for different cowl deflection (C_α). At $C_\alpha=1$ a normal shock is observed in the downstream portion of diffuser, whereas it was not observed for free exit flow (Fig. 8). With increase in C_α , the location of normal shock moves upstream and

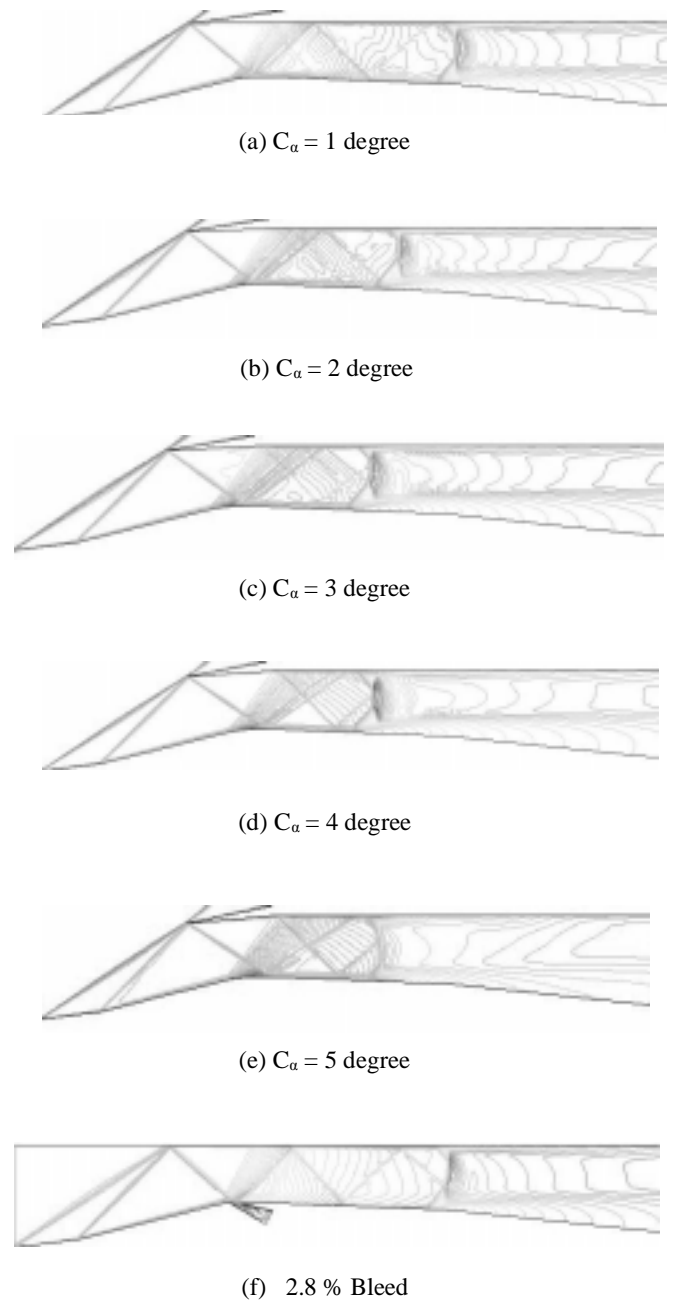


Figure 14. Density contours at various C_α with back pressure and bleed.

leads to subsonic flow downstream of the shock. During the computation for $C_\alpha = 5^\circ$, oscillations in the results were observed which may be due to possibility of shock existing near the throat.

Pressure distribution on the ramp surface at different C_α is presented in Fig. 15. As expected, trends are almost similar to free exit flow up to the location of normal shock. Further downstream the increase in pressure due to shock and diffuser is captured. From these pressure distributions, the location of normal shock wave could be obtained which is presented in Fig.16, indicating the movement of shock upstream with increase in C_α . Similar behaviour was also observed from the density contours presented in Fig.14. The results indicate that at higher C_α , the effect is not predominant, suggesting that use of larger cowl deflection may not be advantageous with back pressure, however this needs to be looked in more details. Figure17 shows the pressure distribution on the cowl inner surface at different (C_α), which also depicts the normal shock movement with C_α .

The performance of intake with back pressure ratio of 7 was obtained adopting similar method adopted for free flow, using the pressure distribution at the exit plane presented in Fig. 18. This indicates more non-uniformity in comparison to free exit flow (Fig. 12), which may be due to the presence of flow separation occurring after the normal shock inside the intake. Considering the profile of pressure distribution, the average pressure recovery has been obtained using the data between $0.5 h_d$ to $0.9 h_d$ only. The pressure recovery obtained at different C_α is presented in Fig. 19. This indicates that at this back pressure the pressure recovery decreases at higher C_α . It may be noted that the method adopted to estimate the overall pressure recovery (averaging data between $0.5 h_d$ - $0.9 h_d$) may not be appropriate and needs more investigation. Computations have been made with back pressure and with bleed of 2.8 per cent near the throat region as done for free exit flow. The computed pressure recovery with this bleed is also shown in Fig.18. The profile is almost

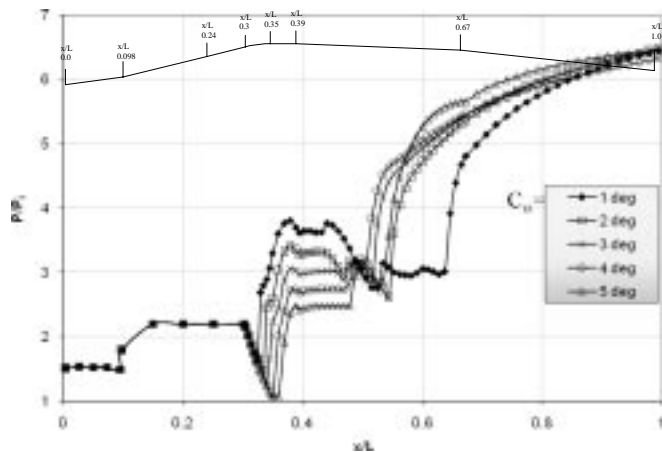


Figure 15. Pressure distribution on ramp at various C_α with back pressure.

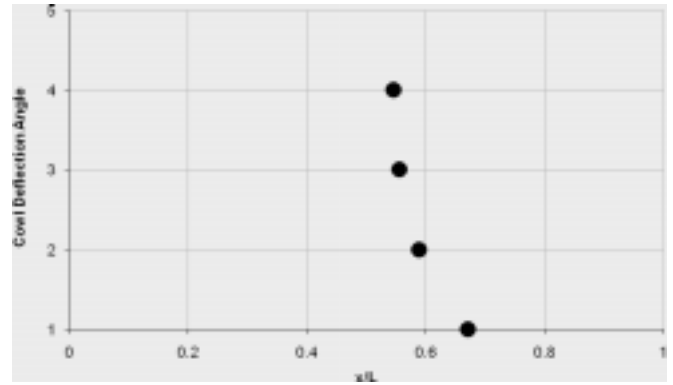


Figure 16. Location of terminal shock with back Pressure.

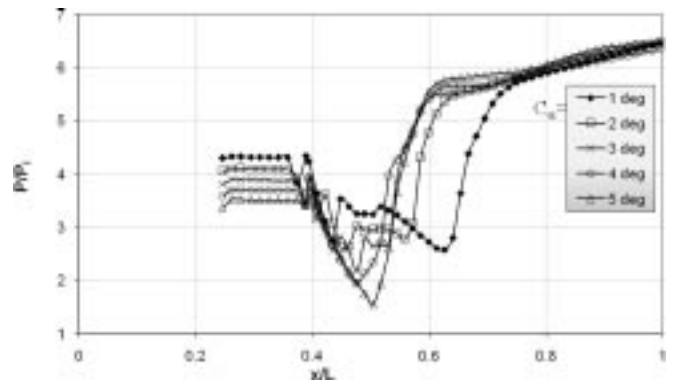


Figure 17. Cowl pressure distribution for various C_α with back pressure exit.

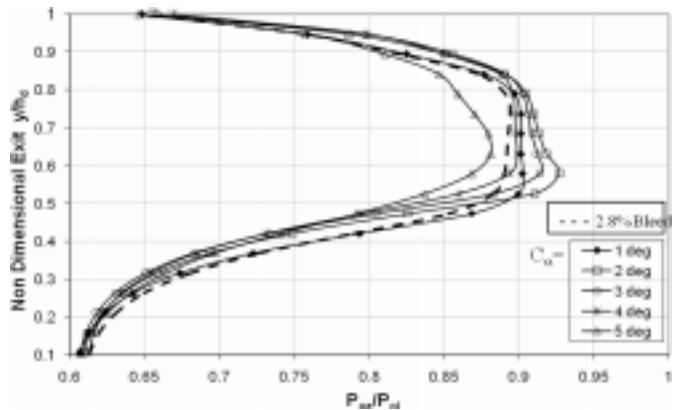


Figure 18. Exit pressure recovery distribution for back pressure.

similar to profile observed at C_α of 3° and 4° . The density contour for this case is presented in Fig.14(f). The average pressure recovery was obtained for all the profiles and presented in Fig.19. The maximum pressure recovery was obtained at around cowl deflection of 2° . The estimated pressure recovery with bleed is found to be about 86.7 per cent, which is in close agreement with the value of 87 per cent reported in Neale and Lamb¹. Comparison indicates that the pressure recovery obtained with 2.8 per cent bleed could be obtained with C_α of the order of 3° . Also it could be observed that at smaller cowl deflection, the performance is better than with bleed. The results

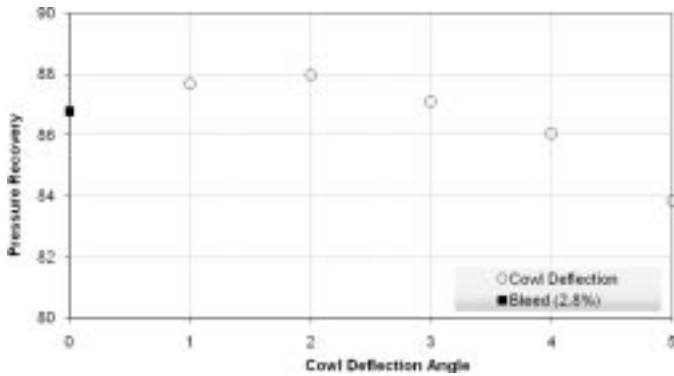


Figure 19. Pressure recovery with back pressure.

obtained from the present computation indicate that, with cowl deflection there is definite improvement in the performance of intake.

8. CONCLUSION

Computations have been made on a two-dimensional mixed compression air intake with design Mach number of 2.2 using the software FLUENT. The computed results indicate good comparison with available experimental and computational results. Effect of cowl deflection angle has been studied to capture the overall flow field and performance of intake for free exit flow and with back pressure. Computations have been also made with bleed. For free exit flow, increase in cowl deflection angle increases the overall performance, however for pressurised exit flow, small cowl deflection angle of the order of 2° leads to improvement in performance. Due to flow separation in the larger area of the intake due to back pressure, the flow gets distorted at the exit plane. It is also observed that improvement in performance with cowl deflection of around 2° is comparable to performance with 2.8 per cent bleed, hence the cowl deflection could be also thought of as an alternative to bleeding.

REFERENCES

1. Neale, M. C. & Lamb, P. S. Tests with a variable ramp intake having combined external / internal compression, and a design Mach number of 2.2. Aeronautical Research Council - CP - 805, 1962.
2. Neale, M. C. & Lamb, P. S. More tests with a variable ramp intake having a design mach number of 2.2. Aeronautical Research Council - CP - 938, 1963.
3. Liou, M.; Hankey, W. L & Mace, J. L. Numerical simulation of a supercritical inlet flow. AIAA Paper-1985-1214.
4. Hsieh, T.; Wardlaw, A. B.; Collins, P. & Coakley, T. Numerical investigation of unsteady inlet flowfields. *AIAA Journal*, 1987, **25**(1), 75-81.
5. Biedron, R. T. & Adamson, T. C. Unsteady flow in a supercritical supersonic diffuser. *AIAA Journal*, 1988, **26**(11), 1336-345.
6. Valorani, M.; Nasuti, F.; Onofri, M. & Buongiorno, C. Optimal supersonic intake design for air collection engines (ACE). *Acta Astronaut.*, 1999, **45**(12), 729-45.
7. Reinartz, B. U.; Herrmann, C. D.; Ballmann, J. & Koschel, W.W. Aerodynamic performance analysis of a hypersonic inlet isolator using computation and experiment. *J. Propul. Power*, 2003, **19**(5), 868-75.
8. Van Wie, D. M.; Kwok, F. T. & Walsh, R. F. Starting characteristics of supersonic inlets, AIAA Paper 96-2914, 1996.
9. Kubota, S.; Tani, K & Masuya, G. Aerodynamic performances of a combined cycle inlet, *J. Propul. Power*, 2006, **22**(4), 900-904.
10. Fisher, S.A.; Neale, M. C. & Brooks, A. J. On the sub-critical stability of variable ramp intakes at mach numbers around 2. National Gas Turbine Establishment Report No. ARC-RM-3711, 1970.
11. Sajben, M.; Bogar, T. J. & Kroutil, J. C. Experimental study of flows in a two-dimensional inlet model. AIAA Paper 83-0176, 1983.
12. Trapier, S.; Duveau, P. & Deck, S. Experimental study of supersonic inlet buzz. *AIAA Journal*, 2006, **44**(10), 2354-365.
13. Coratekin, T.; VanKeuk, J. & Ballmann, J. Preliminary investigations in 2-D and 3-D ramjet inlet design. AIAA Paper-99-2667, 1999.

Contributors



Mr Sudip Das obtained his ME (Space Engg. & Rocketry) from Birla Institute of Technology, Mesra, in 2001. He worked as Graduate Trainee at National Aerospace Laboratories (NAL), Bangalore, during 1998-1999. He joined BIT, Mesra, as Lecturer in 2001, and is presently working as Senior Lecturer in the Department of Space Engineering and Rocketry. He has guided many students for Masters programme and has 39 publications in journals and conference proceedings to his credit. He is a member of Aeronautical Society of India, Institution of Engineers (I), Indian Society for Technical Education, and Society of Fluid Mechanics and Fluid Power. His areas of research are Aerodynamics, CFD, and jet propulsion.



Prof J.K. Prasad obtained his PhD (Aerospace Engg) from Indian Institute of Technology Madras in 1992. He worked as Scientist / Engineer and Project Manager at Vikram Sarabhai Space Centre, Thiruvananthapuram, from 1977 to 2001. He had been to DLR Gottingen, Germany, as Visiting Scientist and CALTECH, USA, as Research Fellow. Currently, he is working as Professor at Department of Space Engineering and Rocketry, BIT, Mesra. He has 65 publications in national and international journals and conference proceedings. His areas of research are aerodynamics, jets, jet interactions, etc.